# Influence of concentration polarization on DNA translocation through a nanopore

Shengjie Zhai and Hui Zhao

Phys. Rev. E **93**, 052409 — Published 18 May 2016

DOI: 10.1103/PhysRevE.93.052409

# The Influence of Concentration Polarization on DNA Translocation through a Nanopore

Shengjie Zhai and Hui Zhao[1]

Department of Mechanical Engineering
University of Nevada, Las Vegas, NV, 89154

**Abstract**

Concentration polarization can be induced by the unique ion-perm selectivity of small nanopores, leading to a salt concentration gradient across nanopores. This concentration gradient can create diffusioosmosis and induce an electric field, affecting ionic currents on DNA that translocates through a nanopore. Here this influence is theoretically investigated by solving the continuum Poisson-Nernst-Planck model for different salt concentrations, DNA surface charge densities, and pores' properties. By implementing the perturbation method, we can explicitly compute the contribution of concentration polarization to the ionic current. The induced electric field by concentration polarization is opposite to the imposed electric field and decreases the migration current and the induced diffusioosmosis can decrease the convection current as well. Our studies suggest that the importance of the concentration polarization can be determined by the parameter $\lambda/G$ where $\lambda$ is the double layer thickness and $G$ is the gap size. When $\lambda/G$ is larger than a critical value, the influence of concentration polarization becomes more prominent. This conclusion is supported by the studies on the dependence of the ionic current on salt concentration and pore's properties, showing that the difference between two models with and without accounting for concentration polarization is larger for low salts and small pores, which correspond to larger $\lambda/G$.

[1] All correspondence should be directed to this author (hui.zhao@unlv.edu)

## 1. Introduction

When a DC voltage bias is imposed across a nanopore merged in an aqueous electrolyte, the ionic current through the pore can be measured using electrophysiological techniques. A DNA molecule can be electrophoretically driven through the nanopore. Since the pore size is sufficiently small, DNA is forced to pass through the nanopore as a linear unfolded strand rather than randomly coiled globule configuration adopted by DNA molecules in free solutions. Presumably nucleobases in a linear fashion would modify the ionic current through the nanopore. It is hypothesized that the sequence of bases in DNA can be recorded by monitoring the current modulations.[1-3] This method examines the electronic signals or relies on physical properties, in contrast to existing paradigms based on chemical techniques. Thus, nanopore DNA sequencing involves no sample amplification, leading to a label-free and single-molecule approach. In addition, the estimated cost of nanopore sequencing of a human genome is in the range of $1,000 which meets the goals set by the National Institute of Health.[4-6] This cost is believed to be sufficiently low to revolutionize genomic medicine.[4,7] All these encouraging benefits of the DNA sequencing stimulated a fast-growing research area related to the nanopore analysis. Although the nanopore sequencing technology has a promising future, most study and research conducted are still at the early stage and many technology related challenges must be resolved before it can be successfully implemented.[7] One of the challenges is the lack of the detailed knowledge of the dynamics of DNA translocation through the nanopore.

It is recognized that the underlying mechanism of DNA translocation through a nanopore is the interplay between electrostatics and hydrodynamics.[8,9] The hydrodynamic coupling between the DNA's counterions and the nanopore, in part, determines the electrophoretic force in DNA translocation. For simple liquids, the continuum framework of hydrodynamics is valid down to

nanoscales. A number of experiments and molecule simulations suggest that there is no significant deviation from the Navier-Stokes equation for confinement around nanometer range.[10-15] Furthermore, the continuum model has a clear advantage: the model describes the translocation process in statistical terms and can be directly compared with an ensemble average determined by experiments. In addition, since the membranes containing nanopores are very thin (~ tens nanometers), the large persistence length of DNA about 50 nm ensures that the DNA segment inside the pore is fully elongated. In other words, the DNA translocates through the nanopore in a linear fashion.[8,16] Experiments indicated that the entropic force responsible for DNA coiling is small compared to electrostatic and hydrodynamic forces when DNA is stretched.[8,17] Thus it is reasonable to approximate a DNA molecule as a rod and neglect entropic forces during the process of the translocation through the nanopore. In fact, a simple continuum model including hydrodynamics and approximating DNA as a rigid rod has revealed remarkable agreements with experimental measurements including translocation time, translocation velocity and force.[8,18-24] In general, the theory is able to explain the data well for larger pores and high salts. However, for smaller nanopores and low salts, the simple theory seems to consistently overestimate the force. In addition, recent experiments consistently observed that the recorded ionic current increases instead of decreasing when the DNA translocates through the nanopore at low salts.[25-27] Such spike-like current increase cannot be quantitatively explained by the simple model.

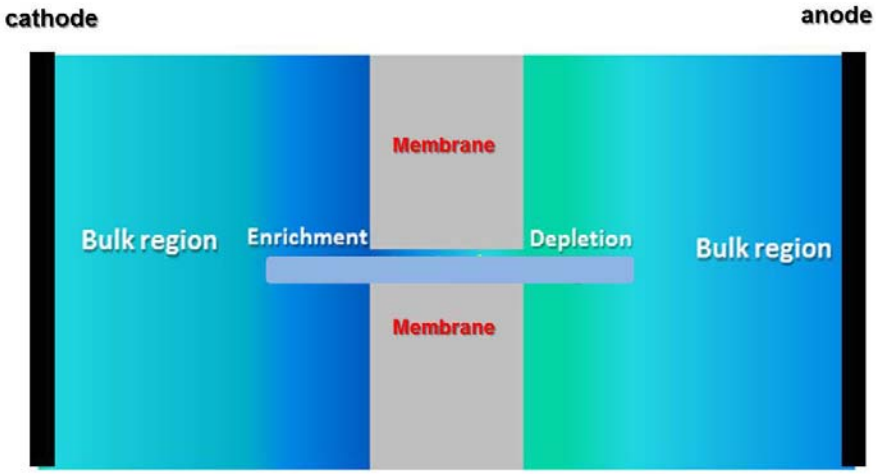


**Figure 1.** (color online) Schematics of concentration polarization due to the DNA translocation inside the nanopore.

The main assumption in the hydrodynamic model in Ghosal[19] is that the bulk concentration assumes to be uniform across the nanopore. However, recent experiments strongly suggest that small-size nanopores have an unique ion-perm selectivity in particular at low salt concentrations since the electrical double layers inside the nanopore overlap.[28] Under the action of an electric field, a nanopore can create a bulk concentration gradient by decreasing the ion concentration at the anodic end and increasing the ion concentration at the cathodic end of the nanopore (**Fig. 1**).[29] The interaction between the electrical double layer and bulk concentration gradient creates an osmotic pressure which induces a diffusio-osmotic flow along the nanopore.[30-34] The concentration gradient will also induce a charged particle to experience a diffusio-phoretic migration from the region of low salt to the region of high salt. Indeed, this migration induced by the external imposed salt gradient has been used to manipulate particles[35-37] or influence DNA translocation through a nanopore.[38,39] In addition, the concentration gradient can induce an electric field, opposite to the applied electric field which can impact ionic current as well.[33] Consider both the discrepancies between the simple model and experimental results and the

importance of concentration polarization at low salt concentrations and small pores. It is worthwhile to investigate the role of concentration polarization in DNA translocation from a fundamental perspective. In addition, since the nanopore sequencing technology relies on recording the ionic current by forcing the DNA translocation through nanopores, from a practical perspective, it is crucial to gain the knowledge of concentration polarization on ionic currents as well. Indeed, recent studies already suggested that concentration polarization is important in DNA translocation.[21,40] However, these studies were still qualitative and their results were not quantitatively compared with existing experimental data. Hence thorough investigations and rigorous comparisons with experiments are necessary to fully understand the importance of concentration polarization in DNA translocation.

In this article, we approximate double-strand DNA molecules as elongated cylinders with uniformly distributed surface charges and employ the continuum Poisson-Nernst-Planck model. Furthermore, we apply the perturbation method to develop two models. One model accounts for the effect of concentration polarization; the other neglects its contribution. Consider the linearity of the perturbed model. The difference between the predictions from these two models yields the contribution of concentration polarization to ionic currents. This approach provides us a direct theoretical tool to isolate the influence of concentration polarization for studies. Our theoretical predictions in Results and Discussion are compared with experimental data to demonstrate that concentration polarization in DNA translocation is important under certain conditions.

## 2. Mathematical Model

We consider a charged elongated rod-shaped particle with radius $a$, length $L$, and two hemispherical caps with radius $a$ at the ends, approximating the double-stranded DNA molecule (**Fig. 2**). The particle is submerged into a binary 1-1 electrolyte with the permittivity $\varepsilon$. Two

reservoirs are separated by an electrically insulated membrane with a thickness $h$. The nanopore with a diameter of $d$ locates on the center of the membrane. Accounting for the axis-symmetry, we use the cylindrical coordinate system $(r,z)$ with its origin at the rod's center.

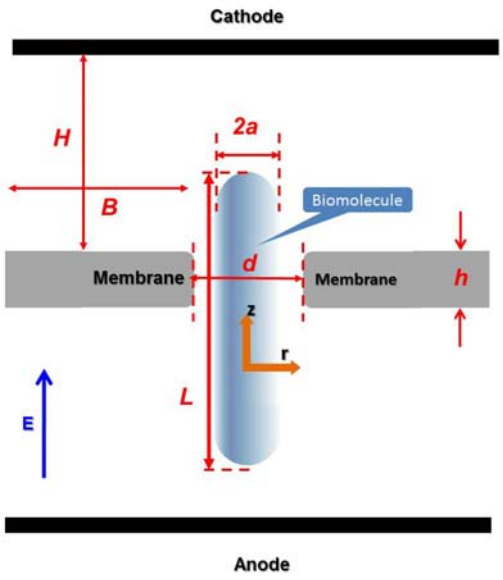


**Figure 2**. (color online) Schematics of the computational model.

A voltage bias is imposed across the membrane. The applied electric field has a profound impact on the dynamics of the DNA. On one hand, the external field exerts an electrostatic force on the charged DNA molecule. On the other hand, since the charged DNA molecule attracts counterions, repels coions, and forms an electric double layer near its surface, the applied electric field acting on the excess ions inside the double layer induces the electro-osmotic flow which, in turn, exerts a hydrodynamic force on the DNA. At low salts and small nanopores, concentration polarization plays a role as well. Hence, the dynamics of the DNA inside a nanopore is controlled by the complex interplay of these electrohydrodynamic effects. To describe these effects, we employ the Poisson-Nernst-Planck model.

Since the Reynolds number associated with DNA translocation is small, advection terms can be neglected, and the fluid flow is modeled with the Stokes equation:

$$-\nabla p-\frac{1}{2\lambda^2}(C_+-C_-)\nabla\varphi+\nabla^2\vec{u}=0\,. \tag{1}$$

In the above, all the variables are dimensionless. The various scales used in the normalization will be given later. $\vec{u}$ is the velocity vector; $p$ is the pressure; $C$ is the ion's concentration; the subscripts (+) and (–) denote, respectively, the cations and the anions; $\varphi$ is the electric potential; $\lambda=\frac{1}{a}\sqrt{\frac{\varepsilon RT}{2F^2C_0}}$ is the dimensionless Debye screening length (normalized with the particle's radius $a$); $C_0$ is the solute's bulk concentration; $R$ is the ideal gas constant; $F$ is the Faraday constant; and $T$ is the temperature.

The mass conservation requires the following continuity equation:

$$\nabla\bullet\vec{u}=0\,. \tag{2}$$

The electric potential $\varphi$ satisfies the Poisson equation:

$$\nabla^2\varphi=-\frac{C_+-C_-}{2\lambda^2}\,. \tag{3}$$

The ionic concentrations satisfy the Nernst-Planck equations:

$$\nabla\bullet\left(-\nabla C_\pm-z_\pm C_\pm\nabla\varphi+PeC_\pm\vec{u}\right)=0\,. \tag{4}$$

In the above, $Pe=\frac{\varepsilon R^2T^2}{\mu DF^2}$; $D$ is the ion's diffusivity; $\mu$ is the solvent's dynamic viscosity.

We use the particle's radius $a$ as the length scale; $RT/F$ as the electric-potential scale; $\varepsilon R^2T^2/(\mu F^2a)$ as the velocity scale; the bulk concentration $C_0$ as the concentration scale;

$\varepsilon R^2T^2/(F^2a^2)$ as the pressure scale; $\varepsilon RT/(Fa)$ as the electric charge scale; and $FDC_0a$ as the ionic current scale.

Non-slip boundary conditions are applied on both the surfaces of the DNA molecule and the nanopore. The electric potential on the DNA's surface obeys $-\partial\phi/\partial n = q$, where $q$ is the surface charge density of the DNA molecule. On the surface of the nanopore, $-\partial\phi/\partial n = q_m$. Zero flux conditions are applied for ionic concentrations on both DNA's and nanopore's surfaces. The top ($Z=H$) and bottom ($Z=-H$) surfaces and the side surface $r=B$ are sufficiently large enough to have little impact on the DNA dynamics inside the nanopore. These surfaces are permeable to fluid flow and have a uniform pressure. The electrolyte solutions at $Z=\pm H$ remain the bulk concentration. The surface at $r=B$ is assumed to be insulated for the ionic fluxes.

The current density

$$\vec{i} = \sum_{\pm} z_{\pm}\left(-\nabla C_{\pm} - z_{\pm}C_{\pm}\nabla\varphi + PeC_{\pm}\vec{u}\right). \tag{5}$$

The total ionic current $I$ can be obtained by integrating Eq. 5 over a lateral cross-sectional area inside the nanopore.

**2.1 The Perturbation Method**

Inside the double layers the applied electric field is typically much smaller than the electric field induced by the surface charge. For example, for a typical nanopore immerged in 100 mM KCl with a biased voltage 120 mV, the electric field generated by the equilibrium double layer of the DNA molecule is about $10^8$ V/m in comparison with $10^6$ V/m generated by the applied electric field. Since the external electric field only slightly disturbs the electric potential and the ions' concentration of the equilibrium double layer, for simplification, we can use a perturbation expansion around the equilibrium double layer:

$$\begin{pmatrix} \varphi \\ C_{\pm} \\ \vec{u} \end{pmatrix} = \begin{pmatrix} \varphi^{(0)} \\ C_{\pm}^{(0)} \\ 0 \end{pmatrix} + \delta \begin{pmatrix} \varphi^{(1)} \\ C_{\pm}^{(1)} \\ \vec{u}^{(1)} \end{pmatrix} + \mathrm{O}(\delta^2) . \tag{6}$$

In the above, we denote the perturbed quantities with the prefix $\delta$. $\delta$ is defined as the ratio between the magnitude of the corresponding external electric field and the electric field of the equilibrium double layer. $\delta \sim 10^{-2}$ for a typical nanopore device. The superscript ($i$) denotes the $i^{\text{th}}$ order expansions in terms of the external electric field. The electrophoretic motion is proportional to the external electric field and can be determined from the first order equations. The use of the perturbation method can significantly simplify numerical simulations and facilitate the computation. Even more importantly, it provides a theoretical tool to explicitly study the influence of concentration polarization on DNA dynamics inside the nanopore as shown later.

**Zeroth Order Approximation**

We assume that $\phi^{(0)}$ and $C_{\pm}^{(0)}$ are, respectively, the equilibrium electric potential and the equilibrium concentrations induced by the surface charge in the absence of an external electric field.

At equilibrium, ions' concentrations $C_{\pm}^{(0)}$ obey the classical Boltzmann distribution:

$$C_{\pm}^{(0)} = e^{\mp \varphi^{(0)}} . \tag{7}$$

The electric potential $\varphi^{(0)}$ satisfies the Poisson-Boltzmann equation:

$$\nabla^2 \varphi^{(0)} = \frac{\sinh(\varphi^{(0)})}{\lambda^2} . \tag{8}$$

The boundary conditions are

$$-\frac{\partial \varphi^{(0)}}{\partial n} = q \tag{9}$$

at the particle's surface and

$$-\frac{\partial \varphi^{(0)}}{\partial n} = q_m \tag{10}$$

at the nanopore's surface.

**First Order Approximation**

The first-order equations are linear in perturbed quantities. After substituting expansions 6 into Eqs. 1-4, the first order equations can be derived:

$$-\nabla p^{(1)} - \frac{1}{2\lambda^2}((C_+^{(0)} - C_-^{(0)})\nabla \varphi^{(1)} + (C_+^{(1)} - C_-^{(1)})\nabla \varphi^{(0)}) + \nabla^2 \vec{u}^{(1)} = 0\,, \tag{11}$$

$$\nabla \bullet \vec{u}^{(1)} = 0\,, \tag{12}$$

$$\nabla^2 \varphi^{(1)} = -\frac{C_+^{(1)} - C_-^{(1)}}{2\lambda^2}\,, \tag{13}$$

and

$$\nabla \bullet \left(-\nabla C_\pm^{(1)} - z_\pm (C_\pm^{(0)} \nabla \varphi^{(1)} + C_\pm^{(1)} \nabla \varphi^{(0)}) + PeC_\pm^{(0)} \vec{u}^{(1)}\right) = 0\,. \tag{14}$$

The first order current density is:

$$\vec{i}^{(1)} = \sum_\pm z_\pm \left(-\nabla C_\pm^{(1)} - z_\pm C_\pm^{(0)} \nabla \varphi^{(1)} - z_\pm C_\pm^{(1)} \nabla \varphi^{(0)} + PeC_\pm^{(0)} \vec{u}^{(1)}\right). \tag{15}$$

**The Model Neglecting Concentration Polarization**

Since concentration polarization is induced by the bulk concentration gradient across the nanopore and there is no concentration gradient in the zeroth order across the nanopore, the

concentration gradient arises from the first order. Hence, in the perturbation model, by letting $C_{\pm}^{(1)} = 0$, the influence of concentration polarization can be effectively removed. Now, the equations become

$$-\nabla p^{(1)} - \frac{1}{2\lambda^2}(C_{+}^{(0)} - C_{-}^{(0)})\nabla\varphi^{(1)} + \nabla^2\vec{u}^{(1)} = 0 \ , \tag{16}$$

and

$$\nabla^2\varphi^{(1)} = 0 \, . \tag{17}$$

Eqs. 12, 16, and 17, forming the new model neglecting concentration polarization, can be solved simultaneously to compute the ionic current without concentration polarization.

Due to the linear nature of the perturbation method, the contribution of concentration polarization can be directly deduced from the predictions of the two models. In this way, the impact of concentration polarization can be explicitly studied, which is an advantage of our modeling approach.

The perturbed equations with corresponding boundary conditions were solved with the finite element software Comsol 3.5 (Comsol 3.5 is a product of Comsol, Sweden). We define the domain as $0 < r < B$ and $-H < z < H$ . We specify $B = 2000$ and $H = 2000$ , which are sufficiently large to assure that the solutions are independent of the size of the computational domain. When *B* and *H* were increased by a factor of 5, the numerically computed variables only varied by less than 1%. To resolve the details of the electric double layer, we used non-uniform elements with dense mesh concentrated next to the particle's surface inside the electric double layer. The mesh was refined a few times to assure that the computational results were mesh-independent.

**3. Results and Discussion**

First, we compute the ionic currents and compare them with experimental data. In experiments, Smeets *et al.*[25] measured the dependence of the ionic current change on KCl salt concentrations ranging from 50 mM to 1 M when 16.5-μm-long double-stranded DNA translocates through a solid-state silicon nitride nanopore with a diameter of 10 nm. Interestingly, they observed that the presence of the DNA in the nanopore can either block the ionic current at high salts, resulting in spike-like decrease or enhance the ionic current at low salts, leading to spike-like increase (**Fig. 3**). The current decrease is attributed to the partial blockage of the pore by the DNA molecule. However, the simple model, neglecting concentration polarization, fails quantitatively at low salts. Kesselheim *et al.* [41] attributed this failure to the reduction of ion mobility due to a surface related molecular drag. In contrast, here we provide an alternative interpretation of this quantitative failure.

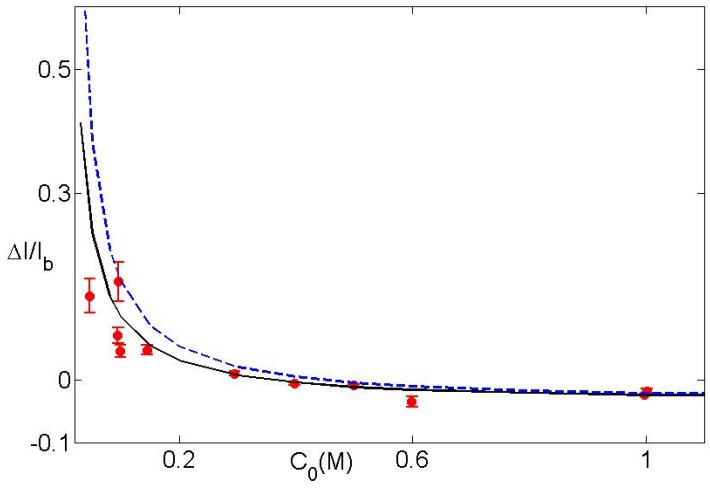


**Figure 3.** (color online) The relative ionic current change $\Delta I / I_b$ as a function of salt concentration when $q_m = 0$ and $q = -0.08\,\mathrm{C/m^2}$. The lines and symbols correspond, respectively, to theoretical predictions and experimental data.[25]

For simulations, the thickness of membrane is given to be 20 nm and the nanopore's diameter is 10 nm as given in experiments. Here we assume that the nanopore is uncharged ($q_m = 0$). The length of the elongated cylinder is 50 nm that is the DNA persistence length. $\Delta I = I - I_b$ is the change of the ionic current from the base current ($I_b$) which is computed from the case in the absence of the DNA molecule. **Fig. 3** depicts the relative ionic current change $\Delta I / I_b$ as a function of salt concentration. The solid line and the dashed line correspond, respectively, to the ones predicted by the model accounting for and neglecting concentration polarization. The symbols are experimental data.[25] In **Fig. 3**, to compare with experiments, $q = -0.08\,\mathrm{C/m^2}$ which is about half of the DNA linear charge density. This effective charge density is consistent with other experimental observations, showing that due to the counterion condensation, the effective charge can be possible half of their original charge density.[42]

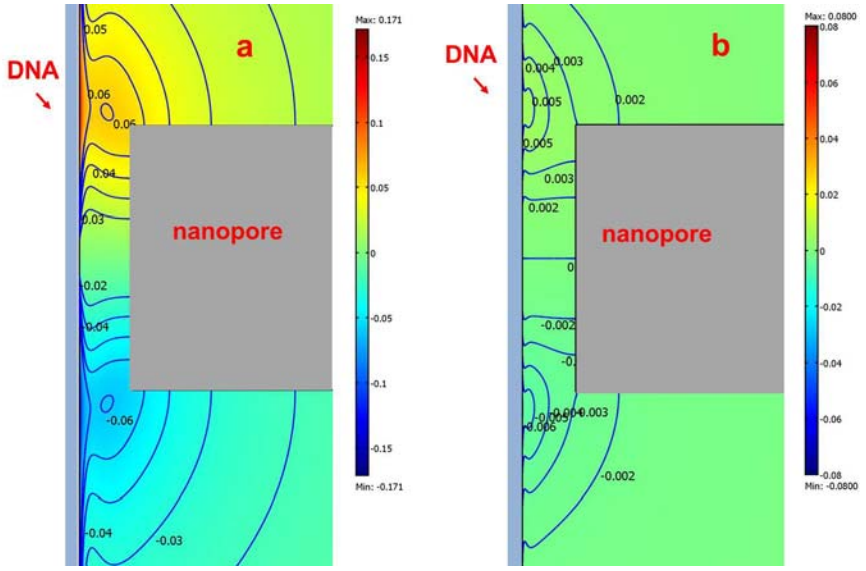


**Figure 4.** (color online) The distributions of the local salt concentration $C^{(1)} = \frac{C_+^{(1)} + C_-^{(1)}}{2}$ when the DNA is inside the nanopore for 50 mM (**a**) and 1 M (**b**). The simulation parameters are the same as Figure 3.

**Fig. 3** demonstrates that the agreements between the model accounting for concentration polarization and the experimental results are quantitatively better than those without considering concentration polarization in terms of predicting the dependence of ionic current on salt concentration at low salts.

Because as we discussed before, the only difference between these two models is the contribution from concentration polarization, it is reasonable to assume that concentration polarization is responsible for the failure of the quantitative predictions at low salts. To illustrate concentration polarization, **Fig. 4** plots, respectively, the distributions of the local salt concentration $C^{(1)} = \frac{C_+^{(1)} + C_-^{(1)}}{2}$ for 50 mM (**Fig. 4a**) and 1 M (**Fig. 4b**). Evidently, the presence of DNA inside the nanopore creates a bulk concentration gradient by decreasing the ion concentration at the anodic end and increasing the ion concentration at the cathodic end of the nanopore. The effect of concentration polarization is much more prominent at low salt concentrations. It also explains that the predictions of two models approach each other at 1 M salt as the concentration gradient is negligible at high salts.

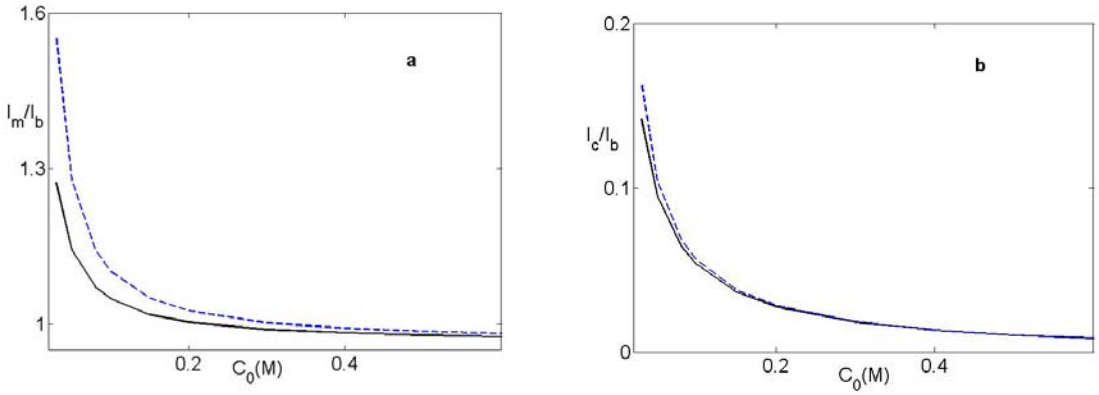


**Figure 5.** (color online) (**a**) The relative migration current $I_m / I_b$ (**b**) the relative convection current $I_c / I_b$ as a function of salt concentration. The lines correspond, respectively, to theoretical predictions of the models with (solid lines) and without (dashed lines) considering concentration polarization.

To understand the impact of concentration polarization on the ionic current, **Fig. 5** depicts the relative migration and convection currents as a function of salt concentration where

$$I_m = \int_A -\sum_{\pm} \left( z_{\pm}^2 C_{\pm}^{(0)} \nabla \varphi^{(1)} + z_{\pm}^2 C_{\pm}^{(1)} \nabla \varphi^{(0)} \right) \bullet dA \,, \tag{18}$$

and

$$I_c = \int_A \sum_{\pm} z_{\pm} Pe C_{\pm}^{(0)} \vec{u}^{(1)} \bullet dA \ . \tag{19}$$

In the above, $A$ is the cross-section at the center of the nanopore ($z$=0). The solid line and the dashed line correspond, respectively, to the ones predicted by the model accounting for and neglecting concentration polarization. It is known that the concentration gradient can generate an electric field which is opposite to the applied electric field,[33] influencing the migration current. Moreover, the induced diffuisoosmostic flow is also opposite to the electro-osmotic flow, affecting the convection current. Interestingly, as shown in **Fig. 5**, both of them decrease the ionic current, compared to the predictions from the simple model. In addition, from Eq. 15, the diffusion caused by the concentration gradient also induces an ionic current. However, our calculations show that the diffusion current is two orders of magnitude smaller than the migration current, indicating that the diffusion current is negligible in terms of influencing the ionic current. Finally, **Fig. 5** suggests that the convection current is much smaller than the migration current. In other words, the qualitative failure of the simple model can be mostly attributed to the reduction of the migration current caused by concentration polarization.

To better understand the conditions when concentration polarization becomes important, in **Fig. 6,** we replot **Fig. 3** in terms of $\lambda/G$ where $\lambda$ is the double layer thickness and $G = (d/2 - a)$ is the gap size. Since $\lambda$ depends on the salt concentration and a lower salt corresponds to a larger $\lambda/G$, **Fig. 6** suggests when $\lambda/G$>0.2, the difference between two predictions from the models with and without concentration polarization becomes not negligible.

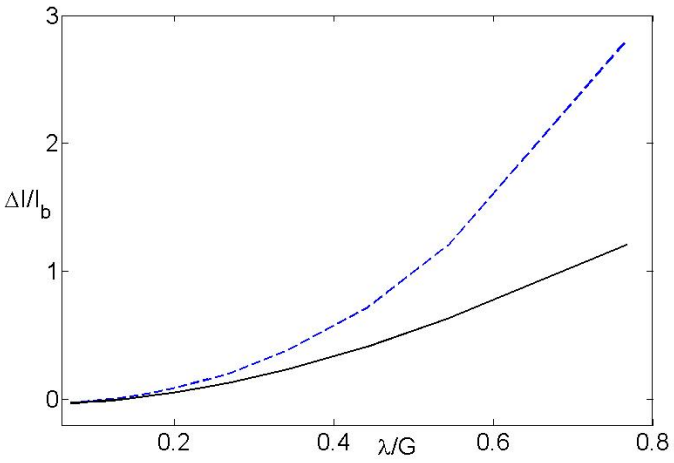


**Figure 6.** (color online) The relative ionic current change $\Delta I / I_b$ as a function of $\lambda/G$. The solid and the dashed lines correspond, respectively, to the predictions with concentration polarization and without concentration polarization.

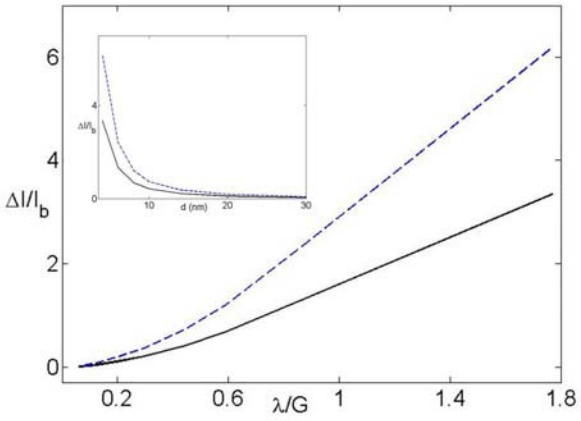


**Figure 7.** (color online) The relative ionic current change $\Delta I / I_b$ as a function of $\lambda/G$ by varying $d$ when the salt concentration is 30 mM. The solid and the dashed lines correspond, respectively, to the predictions with concentration polarization and without concentration polarization. The insert shows $\Delta I / I_b$ as a function of the pore diameter $d$.

To further examine if $\lambda/G$ is a good indicator for the influence of concentration polarization, we compute the relative ionic current change $\Delta I / I_b$ as a function of the nanopore diameter since the nanopore diameter can directly change $G$. **Fig. 7** plots the relative ionic current change $\Delta I / I_b$ as a function of $\lambda/G$ by varying the pore size when the salt concentration is 30 mM and all other conditions remain the same as in **Fig. 3**. The solid and the dashed lines correspond, respectively, to the predictions with and without concentration polarization. Again, $\lambda/G$ is capable of characterizing the importance of concentration polarization. When $\lambda/G$>0.2, the impact of concentration polarization is not negligible. Moreover, the larger $\lambda/G$; the stronger concentration polarization; the bigger difference between two models.

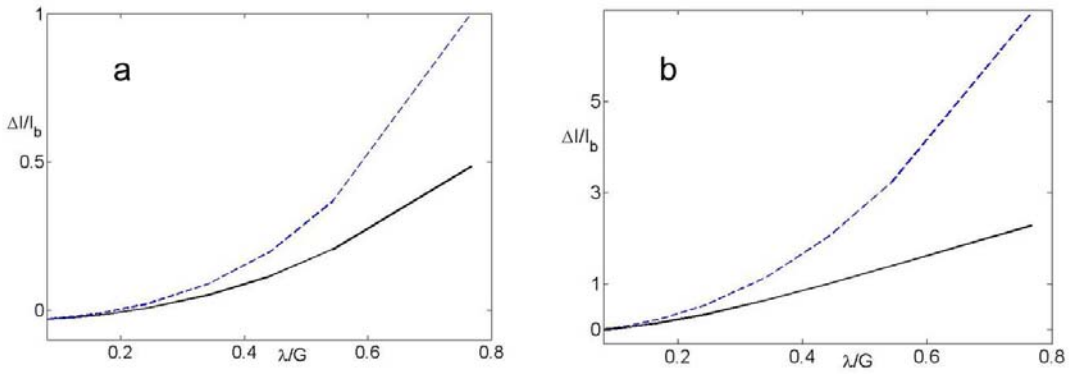


**Figure 8.** (color online) The relative ionic current change $\Delta I / I_b$ as a function of $\lambda/G$ by varying salt concentration for different DNA charge densities: (**a**) $q = -0.04\,\mathrm{C/m^2}$ and (**b**) $q = -0.15\,\mathrm{C/m^2}$. The solid and the dashed lines correspond, respectively, to the predictions with concentration polarization and without concentration polarization.

Next, we examine the impact of the DNA's surface charge density on ionic current change. **Fig. 8** depicts the relative ionic current change $\Delta I / I_b$ as a function of $\lambda/G$ by changing salt concentration for different DNA charge densities: (**a**) $q = -0.04\,\mathrm{C/m^2}$ and (**b**) $q = -0.15\,\mathrm{C/m^2}$. In **Fig. 8**, all the remaining conditions are the same as in **Fig. 3**. Evidently, the magnitude of concentration polarization is controlled by the DNA surface charge. It can be readily understood: a higher surface charge density suggests a larger impact of concentration polarization. Hence, it is not surprising that the discrepancies between two models increase as the DNA surface charge density increases suggested by **Fig. 6** and **Fig. 8**. Interestingly, In addition, **Fig. 8** indicates that the critical value of $\lambda/G$, above which the impact of concentration polarization is not negligible, is less sensitive to $q$.

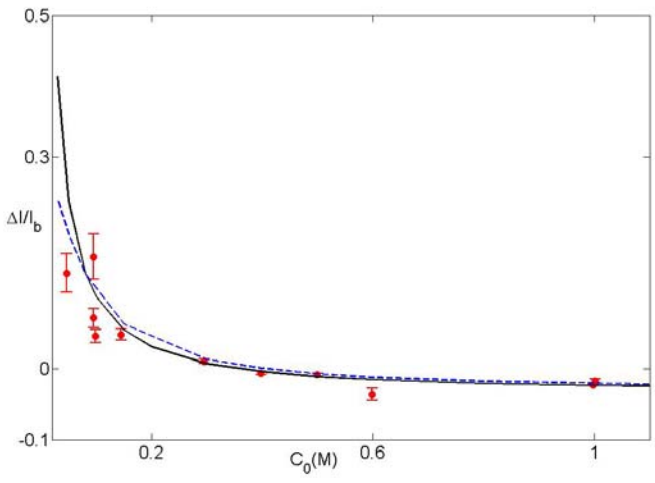


**Figure 9.** (color online) The relative ionic current change $\Delta I / I_b$ as a function of salt concentration. The lines and symbols correspond, respectively, to theoretical predictions and experimental data.[25] The solid line and the dashed line correspond, respectively, to $q_m = 0$ an $q_m = -0.08\,\mathrm{C/m^2}$.

Since the solid-state nanopore is typically negatively charged,[43] it is worthwhile to investigate the effect of the nanopore's surface charge on the ionic current. **Fig. 9** depicts the relative ionic current change $\Delta I / I_b$ as a function of salt concentration. The solid line and the dashed line correspond, respectively, to $q_m = 0$ an $q_m = -0.08\,\mathrm{C/m^2}$, where both predictions are from the model accounting for concentration polarization. **Fig.9** indicates that the charged nanopore further reduces the ionic current at low salts. It can be readily understood: concentration polarization is caused by the unique ion-perm selectivity of the nanopore and the magnitude of this selectivity is controlled by the surface charge. In other words, the charged nanopore contributes to the concentration polarization as well. The higher the surface charge; the larger the concentration polarization. Hence it is not surprising that the ionic current is reduced with charged nanopores at low salts. As witnessed in **Fig. 9**, for charged nanopores, the agreements between experimental data and predictions further improve at low salts.

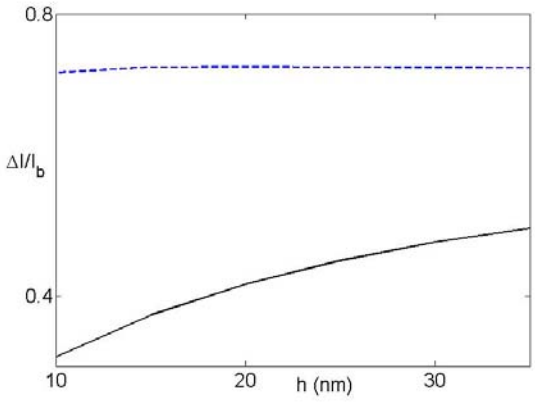


**Figure 10.** (color online) The relative ionic current change $\Delta I / I_b$ as a function of the nanopore thickness when the salt concentration is 30 mM, $d = 10\,\mathrm{nm}$, $q = -0.08\,\mathrm{C/m^2}$, and $q_m = 0$. The solid and the dashed lines correspond, respectively, to the predictions with concentration polarization and without concentration polarization.

Finally, we examine the impact of the nanopore thickness on ionic current change. **Fig. 10** plots the relative ionic current change $\Delta I / I_b$ as a function of the nanopore thickness when the salt concentration is 30 mM, the diameter of the nanopore is 10 nm, $q = -0.08\,\mathrm{C/m^2}$, and $q_m = 0$. The solid and the dashed lines correspond, respectively, to the predictions with concentration polarization and without concentration polarization. Since the concentration polarization is determined by the concentration gradient, a thinner nanopore indicates a larger concentration gradient, resulting in a higher reduction of the ionic current as evidenced in **Fig. 10**.

## 4. Conclusions

Due to the ion-perm selectivity of small-size nanopores, the applied electric field can cause ion depletion at one end and ion enrichment at the other end of the nanopore, developing a bulk concentration gradient across the nanopore termed concentration polarization. The bulk concentration gradient induces an electric field, modifying the ionic current. Concentration polarization becomes more important at small nanopores and low salt concentrations. For DNA sequencing, smaller nanopores are preferable. In addition, consider that ionic currents are crucial to the DNA sequencing technique. The impact of concentration polarization clearly deserved our attentions.

In this article, the influence of concentration polarization on ionic currents was theoretically investigated for different salt concentrations, different DNA surface charge densities and different-property nanopores. One advantage of our approach is that by using the perturbation method, we can explicitly deduce the contribution of concentration polarization to the ionic current. In other words, this approach allowed us to isolate concentration polarization from other important factors governing DNA translocation to better understand the conditions where concentration polarization is significant.

Our studies identified a parameter $\lambda/G$ where $\lambda$ is the double layer thickness and $G$ is the gap size. When $\lambda/G$ is larger than a critical value, the influence of concentration polarization needs to be taken into account for accurately predicting ionic currents. Large $\lambda/G$ typically correspond to low salt concentrations and small nanopores.

The theoretical predictions were compared with experimental data of the translocation of double-stranded DNA molecules through nanopores with a single fitting parameter, DNA effective surface charge density. The model considering concentration polarization quantitatively describes the dependence of ionic current on the salt concentration. This suggests the importance of concentration polarization in the dynamics of DNA translocation, which is necessary to be accounted in modeling for both experimental interpretation and guiding design, in particular, for small pores and low salts.

The main strength of the model used here is the continuum framework, making it possible be directly compared with the experimental measurements like the ionic current. The comparisons between the predictions by the Brownian dynamics model and those from the continuum model suggested that when the double layer thickness is smaller than the nanopore's size, the discrepancies between them are not significant.[44] In our simulations, the double layer thickness ranges from 0.1 nm to 2 nm which is smaller than the nanopore radius studied here (> 3 nm). Since the double layer thickness depends on the salt concentration, for solid-state nanopores, when the bulk concentration is larger than tens mM which is the typical salt concentration used in these experiments, our model is adequate to describe the DNA translocation dynamics through the nanopore and can serve as a design tool. Indeed, a similar continuum model has suggested that nanopores can be used to sort DNA fragments based on their size by controlling a gate membrane electrode.[45]

Although the discussions in this manuscript are about the impact of concentration polarization on ionic currents associated with DNA translocation through nanopores, the main conclusion is also applicable for open charged nanopores: the influence of concentration polarization is not negligible for smaller charged nanopores at low salts and the higher the surface charge of the nanopore is; the larger impact of concentration polarization is. Consider that biological channels are charged and have smaller diameters. Our results suggest that concentration polarization may play a role in ion transport within biological channels as well, which can find important applications such as drug delivery.

**Acknowledgment**

We thank the referee for pointing out an error in computing the ionic current from the simple model in the early version. The work described was supported by Grant Number R03HG006562 from the National Human Genome Research Institute. The content is solely the responsibility of the authors and does not necessarily represent the official views of the National Human Genome Research Institute or the National Institutes of Health.

**Reference**


[1] J.J. Kasianowicz, E. Brandin, D. Branton, and D.W. Deamer, Proc. Natl. Acad. Sci. USA **93**, 13770 (1996).

[2] S.G. Lemay, ACS Nano **3**, 775 (2009).

[3] H. Bayley, Curr. Opin. Chem. Biol. **10**, 628 (2006).

[4] J. Clarke, H.C. Wu, L. Jayasinghe, A. Patel, S. Reid, and H. Bayley, Nat. Nanotechnol. **4**, 265 (2009).

[5] D. Ryan, M. Rahimi, J. Lund, R. Mehta, and B.A. Parviz, Trends Biotechnol. **25**, 385 (2007).

[6] J.A. Schloss, Nat. Biotechnol. **26**, 1113 (2008).

[7] D. Branton, D.W. Deamer, A. Marziali, H. Bayley, S.A. Benner, T. Butler, M. Di Ventra, S. Garaj, A. Hibbs, X.H. Huang, S.B. Jovanovich, P.S. Krstic, S. Lindsay, X.S.S. Ling, C.H. Mastrangelo, A. Meller, J.S. Oliver, Y.V. Pershin, J.M. Ramsey, R. Riehn, G.V. Soni, V. Tabard-Cossa, M. Wanunu, M. Wiggin, and J.A. Schloss, Nat. Biotechnol. **26**, 1146 (2008).

[8] S. van Dorp, U.F. Keyser, N.H. Dekker, C. Dekker, and S.G. Lemay, Nat. Phys. **5**, 347 (2009).

[9] O.A. Hickey, C. Holm, J. L. Harden, and G.W. Slater, Phys. Rev. Lett. **105**, 148301 (2010).

[10] L. Bocquet and J.L. Barrat, Soft Matter **3**, 685 (2007).

[11] L. Bocquet and E. Charlaix, Chem. Soc. Rev. **39**, 1073 (2010).

[12] H. Daiguji, Chem. Soc. Rev. **39**, 901 (2010).

[13] U. Raviv and J. Klein, Science **297**, 1540 (2002).

[14] W. Sparreboom, A. van den Berg, and J.C.T. Eijkel, Nat. Nanotechnol. **4**, 713 (2009).

[15] W. Sparreboom, A. van den Berg, and J.C.T. Eijkel, New J. Phys. **12**, 015004 (2010).

[16] C.T.A. Wong and M. Muthukumar, J. Chem. Phys. **126**, 164903 (2007).

[17] M. Wang, H. Yin, R. Landick, J. Gelles, and S. Block, Biophys. J. **72**, 1335 (1997).

[18] S. Ghosal, Phys. Rev. E **74**, 041901 (2006).

[19] S. Ghosal, Phys. Rev. Lett. **98**, 238104 (2007).

[20] S. Ghosal, Phys. Rev. E **76**, 061916 (2007).

[21] H. Liu, S. Qian, and H.H. Bau, Biophys. J. **92**, 1164 (2007).

[22] M. van den Hout, I.D. Vilfan, S. Hage, and N. H. Dekker, Nano Lett. **10**, 701 (2010).

[23] U.F. Keyser, S. van Dorp, and S.G. Lemay, Chem. Soc. Rev. **39**, 939 (2010).

[24] L. Galla, A.J. Meyer, A. Spiering, A. Sichka, M. Mayer, A.R. Hall, P. Reimann, and D. Anselmetti, Nano Lett. **14**, 4176 (2014).

[25] R.M.M. Smeets, U.F. Keyser, D. Krapf, M. Wu, N.H. Dekker, and C. Dekker, Nano Lett. **6**, 89 (2006).

[26] H. Chang, F. Kosari, G. Andreadakis, M.A. Alam, G. Vasmatzis, and R. Bashir, Nano Lett. **4**, 1551 (2004).

[27] R. Fan, R. Karnik, M. Yue, D. Li, A. Majumdar, and P. Yang, Nano Lett. **5**, 1633 (2005).

[28] S.J. Kim, Y.C. Wang, J.H. Lee, H. Jang, and J. Han, Phys. Rev. Lett. **99**, 044501 (2007).

[29] T.A. Zangle, A. Mani, and J.G. Santiago, Chem. Soc. Rev. **39**, 1014 (2010).

[30] J.L. Anderson, Annu. Rev. Fluid Mech. **21**, 61 (1989).

[31] A. Ajdari and L. Bocquet, Phys. Rev. Lett. **96**, 186102 (2006).

[32] R.J. Hill, J. Chem. Phys. **124**, 014901 (2006).

[33] H.J. Keh and H. C. Ma, Langmuir **21**, 5461 (2005).

[34] H.C. Ma and H.J. Keh, J. Colloid Interface Sci. **298**, 476 (2006).

[35] B. Abecassis, C. Colttin-Bizonne, C. Ybert, A. Ajdari, and L. Bocquet, Nat. Mater. **7**, 785 (2008).

[36] D.C. Prieve, Nat. Mater. **7**, 769 (2008).

[37] D.C. Prieve, J.L. Anderson, J.P. Ebel, and M.E. Lowell, J. Fluid Mech. **148**, 247 (1984).

[38] T. Chou, J. Chem. Phys. **131**, 034703 (2009).

[39] M. Wanunu, W. Morrison, Y. Rabin, A. Y. Grosberg, and A. Meller, Nat. Nanotechnol. **5**, 160 (2010).

[40] S. Das, P. Dubsky, A. van den Berg, and J.C.T. Eijkel, Phys. Rev. Lett. **108**, 138101 (2012).

[41] S. Kesselheim, W. Muller, and C. Holm, Phys. Rev. Lett. **112**, 018101 (2014).

[42] J.A. Schellman and D. Stigter, Biopolymers **29**, 1415 (1977).

[43] D.P. Hoogerheide, S. Garaj, and J.A. Golovchenko, Phys. Rev. Lett. **102**, 256804 (2009).

[44] B. Corry, S. Kuyucak, and S. Chung, Biophys. J. **78**, 2364 (2000).

[45] S. Getfert, T. Tows, and P. Reimann, Phys. Rev. E **87**, 062710 (2013).